

MEMS Tutorial: Nonlinearity in Micromechanical Resonators

In this tutorial, we cover the effect of nonlinear spring forces on (micro)resonators. The motivation of analysis is: i. to understand the nonlinear effects observed with real resonators and ii. to estimate the maximum vibration amplitude where vibrations are *almost linear*. Knowing the range for linear vibrations sets the dynamic range for resonators. On the lower end, the usable range is limited by intrinsic noise in the MEMS system. The upper end is limited by the resonator power handling capacity which, as we'll see shortly, is limited by nonlinear effects. The analysis in this tutorial follows closely to Landau [2] but the presentation has been slightly modernized.

Preliminaries

Before going into the analysis of nonlinear resonators, it is useful to review the familiar harmonic resonator shown in Figure 1. The equation of motion for a mass-spring-dash pot is

$$m \frac{\partial^2 x}{\partial t^2} + \gamma \frac{\partial x}{\partial t} + kx = F_\omega \cos \omega t, \quad (1)$$

where x is the motion of the mass m , γ is the damping coefficient, k is the spring constant, and F_ω is the magnitude of the forcing term at frequency ω . It is helpful to define the resonant frequency $\omega_0 = \sqrt{k/m}$ and the quality factor $Q = \omega_0 m / \gamma$. Solving Equation (1) for the amplitude of vibrations gives

$$|X| = \frac{F_\omega / m}{\sqrt{(\omega^2 - \omega_0^2)^2 + (\omega \omega_0 / Q)^2}}. \quad (2)$$

Figure 1 sketches the resonator frequency response given by Equation (2). As the focus of this tutorial is on resonators, we'll concentrate on the response near the resonance frequency.

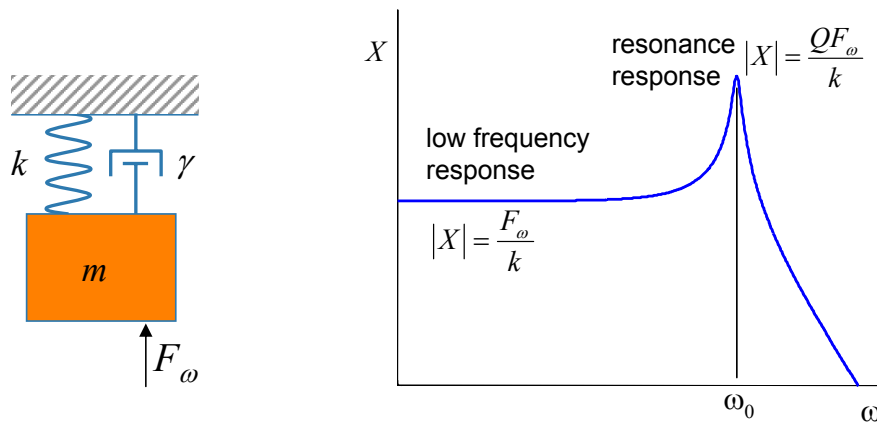


Figure 1. Harmonic resonator and its frequency response.

Nonlinear spring forces

In general, the nonlinear spring force can be written as

$$F = -kx - k_1x^2 - k_2x^3 + O(x^4), \quad (3)$$

where k is the normal linear spring constant, k_1 and k_2 are the first and second order corrections, respectively, and x is the spring displacement. With the nonlinear spring constant, the equation of motion for the mass-spring-dash pot resonator becomes

$$m \frac{\partial^2 x}{\partial t^2} + \gamma \frac{\partial x}{\partial t} + kx + k_1x^2 + k_2x^3 = F_\omega \cos \omega t. \quad (4)$$

Equation (4) is solved in two parts: First, in the next section, the unforced and undamped vibrations are analyzed. Next, the obtained solution is used to approximate forced vibrations.

Unforced vibrations

Setting $\gamma = 0$ and $F_\omega = 0$ in Equation 4, we obtain

$$m \frac{\partial^2 x}{\partial t^2} + kx + k_1x^2 + k_2x^3 = 0. \quad (5)$$

From physics, we expect the unforced, undamped harmonic oscillator to oscillate infinitely with constant amplitude at the resonance frequency ω_0 . The nonlinear terms will change the oscillation frequency to ω'_0 . Moreover, the oscillation frequency ω'_0 will depend on oscillation amplitude due to k_1x^2 and k_2x^3 terms in Equation (5). To obtain this relationship we carry out perturbation analysis around the linear oscillation frequency ω_0 . After all we are interested in almost linear systems! Dividing by m and making the change of variables in Equation (5) as

$$\begin{aligned} k_1 &= \varepsilon \alpha m \\ k_2 &= \varepsilon^2 \beta m \\ \omega'_0 t &= \tau \end{aligned} \quad (6)$$

gives

$$\omega_0^2 \frac{\partial^2 x}{\partial \tau^2} + \omega_0^2 x + \varepsilon \alpha x^2 + \varepsilon^2 \beta x^3 = 0. \quad (7)$$

Notice that in Equation (6) the first-order correction to spring constant k_1 is proportional to ε while the second-order correction k_2 is proportional to ε^2 . This approach provides a convenient way to group the perturbation terms by their order. Next, we substitute $\omega'_0 = \omega_0 + \varepsilon \omega_1 + \varepsilon^2 \omega_2$ and $x = x_0 + \varepsilon x_1 + \varepsilon^2 x_2$ to Equation (7) and group the terms in powers of ε :

$$\begin{aligned} &\omega_0^2 \frac{\partial^2 x_0}{\partial \tau^2} + \omega_0^2 x_0 \\ &+ \varepsilon \left[\omega_0^2 \frac{\partial^2 x_1}{\partial \tau^2} + \omega_0^2 x_1 + \alpha x_0^2 + 2\omega_0 \omega_1 \frac{\partial^2 x_0}{\partial \tau^2} \right] \\ &+ \varepsilon^2 \left[\omega_0^2 \frac{\partial^2 x_2}{\partial \tau^2} + \omega_0^2 x_2 + 2\alpha x_0 x_1 + \beta x_0^3 + (\omega_1^2 + 2\omega_0 \omega_2) \frac{\partial^2 x_0}{\partial \tau^2} + 2\omega_0 \omega_2 \frac{\partial^2 x_1}{\partial \tau^2} \right] \\ &+ O(\varepsilon^3) = 0. \end{aligned} \quad (8)$$

For Equation (8) to be satisfied for $\varepsilon \neq 0$, the following Equations must be satisfied:

$$\omega_0^2 \frac{\partial^2 x_0}{\partial \tau^2} + \omega_0^2 x_0 = 0, \quad (9)$$

$$\omega_0^2 \frac{\partial^2 x_1}{\partial \tau^2} + \omega_0^2 x_1 + \alpha x_0^2 + 2\omega_0 \omega_1 \frac{\partial^2 x_0}{\partial \tau^2} = 0, \quad (10)$$

and

$$\omega_0^2 \frac{\partial^2 x_2}{\partial \tau^2} + \omega_0^2 x_2 + 2\alpha x_0 x_1 + \beta x_0^3 + (\omega_1^2 + 2\omega_0 \omega_2) \frac{\partial^2 x_0}{\partial \tau^2} + 2\omega_0 \omega_2 \frac{\partial^2 x_1}{\partial \tau^2} = 0. \quad (11)$$

Equation (9) is just the harmonic resonator and has the solution

$$x_0 = X_0 \cos \tau. \quad (12)$$

Substituting Equation (12) to (10) gives

$$\omega_0^2 \frac{\partial^2 x_1}{\partial \tau^2} + \omega_0^2 x_1 = -\frac{1}{2} \alpha X_0^2 (1 + \cos 2\tau) + 2\omega_0 \omega_1 X_0 \cos \tau. \quad (13)$$

The resonant term¹ $2\omega_0 \omega_1 X_0 \cos \tau$ on the right side of Equation (13) would result in x_1 growing infinitely. This is physically not possible as no energy is pumped into the resonator system. Thus, we require the resonant term to be zero leading to $\omega_1 = 0$. Solving Equation (13) then leads to

$$x_1 = -\frac{3\alpha}{6\omega_0^2} X_0^2 + \frac{\alpha}{6\omega_0^2} X_0^2 \cos 2\tau. \quad (14)$$

We thus have two additional frequency components due to the first-order corrections: a dc-term and a higher harmonic at twice the oscillation frequency. Substituting Equations (12) and (14) to (11) gives

$$\omega_0^2 \frac{\partial^2 x_2}{\partial \tau^2} + \omega_0^2 x_2 = -\left[-\frac{5\alpha^2}{6\omega_0^2} X_0^3 + \frac{3\beta}{4} X_0^3 - 2\omega_0 \omega_2 X_0 \right] \cos \tau - \left[\frac{\alpha^2}{6\omega_0^2} X_0^3 + \frac{\beta}{4} X_0^3 \right] \cos 3\tau \quad (15)$$

We again require that the resonant term is zero giving

$$\omega_2 = \left[-\frac{5\alpha^2}{12\omega_0^3} + \frac{3\beta}{8\omega_0} \right] X_0^2. \quad (16)$$

Solving Equation (15) then leads to

$$x_2 = \left[\frac{\alpha^2}{24\omega_0^4} + \frac{\beta}{16\omega_0^2} \right] X_0^3 \cos \tau + \left[\frac{\alpha^2}{48\omega_0^4} + \frac{\beta}{32\omega_0^2} \right] X_0^3 \cos 3\tau. \quad (17)$$

Due to the second-order correction, we again have two additional components to motion: an additional term at oscillation frequency and a term at three times the oscillation frequency. The additional term at oscillation frequency is a finger print of odd-order nonlinearity that is very detrimental in communication systems as it causes aliasing of noise and interference to signal band.

To summarize this section, the nonlinear spring constant change the resonance frequency of the resonator as

$$\omega'_0 = \omega_0 + \varepsilon^2 \omega_2 = \omega_0 + \kappa X_0^2, \quad (18)$$

where

$$\kappa = \frac{3k_2}{8k} \omega_0 - \frac{5k_1^2}{12k^2} \omega_0. \quad (19)$$

Equation (18) will be used in the next section to analyze forced vibrations of damped resonator.

¹The resonant excitation terms are sometimes referred to as the secular terms.

Nonlinear forced vibrations

As we saw in the previous section, the main effect nonlinear springs were to change the resonant frequency of the resonator. Therefore, to analyze forced vibrations, make use of Equation (18) substitute $\omega_0 \rightarrow \omega'_0$ to Equation (1). The time harmonic vibration amplitude near the resonance is then given by

$$X_0 = \frac{F\omega_0/m}{\sqrt{(\omega^2 - \omega_0'^2)^2 + (\omega\omega_0'/Q)^2}}, \quad (20)$$

where $\omega'_0 = \omega_0 + \kappa X_0^2$ from the previous section. Equations (18), (19) and (20) show that due to a positive or negative k_1 , the peak-frequency given by $\omega = \omega'_0$ shifts to a lower frequency with an increasing vibration amplitude X_0 as illustrated in Figure 2. Similarly, a negative k_2 results in the peak-frequency shifting to a lower frequency while a positive k_2 results in a higher peak-frequency.

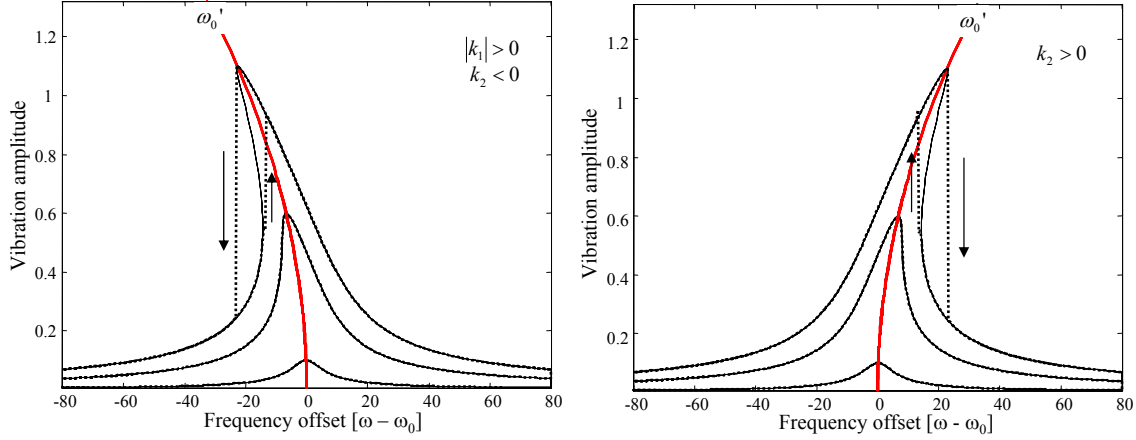


Figure 2. Simulated (dotted lines) and analytical (solid lines) resonator amplitude-frequency response curves around the resonance frequency. Depending on the spring constant, the peak-frequency can shift to either higher or lower frequency. At large vibration amplitudes the response shows hysteresis.

A useful measure of the maximum vibration amplitude is obtained by calculating the bifurcation point x_b shown in Figure 3. At higher excitation levels, the amplitude-frequency relationship is no longer a single valued function and shows hysteresis. Thus, the maximum vibration amplitude before hysteresis x_c can be used to estimate the limit for linear operation.

To obtain an analytical estimate for the bifurcation we write $\Delta\omega = \omega - \omega_0$ and make use of the approximations $(\omega_0 + \Delta\omega)^2 - \omega_0'^2 = (\omega_0 + \Delta\omega + \omega'_0)(\omega_0 + \Delta\omega - \omega'_0) \approx 2\omega_0(\Delta\omega - \kappa X_0^2)$ and $(\omega_0 + \Delta\omega)\omega'_0 \approx \omega_0^2$ to write Equation (20) as

$$X_0^2 = \frac{F^2/m^2}{4\omega_0^2 [(\Delta\omega_0 - \kappa X_0^2)^2 + \omega_0^2/4Q^2]} \quad (21)$$

or

$$X_0^2 4\omega_0^2 [(\Delta\omega_0 - \kappa X_0^2)^2 + \omega_0^2/4Q^2] = F^2/m^2. \quad (22)$$

As Figure 3 indicates, at bifurcation point the slope $\partial X_0/\partial\Delta\omega = \infty$. Deriving Equation (22), solving for $\partial X_0/\partial\Delta\omega$, and requiring that denominator is zero (to give $\partial X_0/\partial\Delta\omega = \infty$) leads to

$$X_0^2 = \frac{4Q^2\Delta\omega\kappa \pm \sqrt{4Q^4\Delta\omega^2\kappa^2 - 3Q^2\kappa^2\omega_0^2}}{6Q^2\kappa^2}. \quad (23)$$

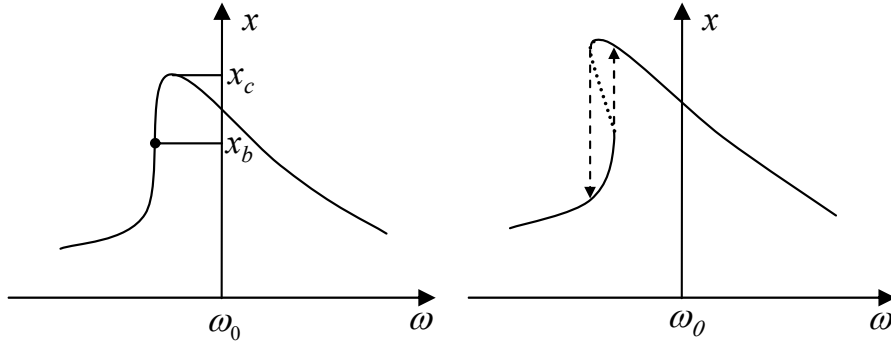


Figure 3. At bifurcation point, the slope of the amplitude-frequency curve becomes infinite. After bifurcation, the amplitude-frequency curve has unstable region (dotted line) resulting in frequency hysteresis. Notice also that after bifurcation, the amplitude-frequency curve is no longer single valued function.

For Equation (23) to be the bifurcation point, it has to be single valued. Requiring that $4Q^4\Delta\omega^2\kappa^2 - 3Q^2\kappa^2\omega_0^2 = 0$ gives

$$\Delta\omega = \pm \frac{\sqrt{3}\omega_0}{2Q} \quad (24)$$

at bifurcation, where the positive and negative sign are for the positive and negative κ , respectively. Substituting back to (20) gives

$$x_b = \sqrt{\frac{\omega_0}{\sqrt{3}Q|\kappa|}} \quad (25)$$

for the bifurcation point.

As indicated in Figure 3, the critical vibration amplitude (or the greatest vibration amplitude) is slightly higher than the vibration amplitude at the bifurcation point. It is obtained by substituting Equations (24) and (25) to Equation (20) and solving for the force. The amplitude of vibrations at resonance due to this force is

$$x_c = \sqrt{\frac{4\omega_0}{3\sqrt{3}Q|\kappa|}}. \quad (26)$$

As Equation (26) shows, increasing the quality factor *lowers* the critical vibration amplitude x_c as the resonator is made more susceptible to nonlinearities.

Implications

As we have seen, the maximum linear vibration amplitude is limited by nonlinearity and the nonlinear effects therefore set the upper limit to the resonator dynamic range (the lower limit being set by noise). The energy stored in the resonator at the critical vibration amplitude x_c is

$$E_c = \frac{1}{2}k_0x_c^2 \quad (27)$$

and the drive level defined as power dissipated in the resonator is

$$P_c = \frac{\omega_0 E_c}{Q}. \quad (28)$$

Equation (28) also gives the maximum output power that can be obtained from the resonator²

Clamped-clamped beam example

To demonstrate the results of this tutorial, we'll consider the clamped-clamped beam resonator shown in Figure 4. As is typical in MEMS, the spring forces have both mechanical and electrical origin. We therefore write the spring constant as $k = k_m + k_e$, $k_1 = k_{m1} + k_{e1}$, and $k_2 = k_{m2} + k_{e2}$ where m and e refer to mechanical and electrical origin. The mechanical spring constant is obtained from the large deformation analysis. Typically, finite element simulations are used but for tutorial purposes, we use the first-order approximation for the spring constant given by

$$\begin{aligned} k_{m1} &= 0 \\ k_{m2} &= \frac{k_m}{\sqrt{2}w^2} \end{aligned} \quad (29)$$

As Equation (29) indicates, the restoring force increases with displacement. This is analogous to a string anchored from both ends: increasing the spring tension increases the restoring force. Similarly, as the beam is displaced, it goes into tension giving rise to additional restoring force.

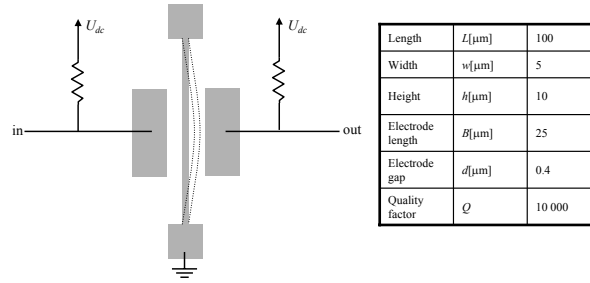


Figure 4. Clamped-clamped beam example.

The electrical nonlinearity arises from the inverse relationship between displacement and parallel plate capacitance. The spring constants are obtained as Taylor series expansion of the electrostatic force giving

$$F = \frac{U_{dc}^2}{2} \frac{\partial C}{\partial x} = \frac{U_{dc}^2 C_0}{2d} \left(1 + \frac{2}{d}x + \frac{3}{d^2}x^2 + \frac{4}{d^3}x^3 + O(x^4) \right), \quad (30)$$

where C_0 is the initial gap capacitance. The first term is the dc-force term and the spring constant is recognized from the higher order terms as

$$\begin{aligned} k_e &= -\frac{U_{dc}^2 C_0}{d^2} \\ k_{e1} &= \frac{3}{2d} k_e \\ k_{e2} &= \frac{2}{d^2} k_e \end{aligned} \quad (31)$$

Notice that the linear electrostatic spring is negative thus lowering the resonator resonance frequency.

Figure 5 shows the analytical and simulated responses at different bias voltages. At low voltages, the mechanical spring constant dominates and the resonant peak shifts to a higher frequency. At higher bias voltages, the capacitive nonlinearity dominates, and the peak frequency tilts towards lower frequencies³. Also notice that the resonance frequency too changes to a lower frequency with increasing bias voltage. A keen

²Remember: for the optimal power matching, the source and load resistances are equal and same power is dissipated in the source and load.

³To first order, we can even compensate the mechanical nonlinearity with capacitive nonlinearity!

eye may notice that that in case of capacitive nonlinearity, there is small deviation between the simulated and theoretical curves. This is due to fact that we have kept terms only to third-order in Equation (30). Keeping terms to $O(x^5)$ would accurately reproduce the capacitive nonlinearity to hysteresis limit⁴. However, Equations (25) and (26) still give a reasonably good order-of-magnitude estimation of the maximum vibration amplitude.

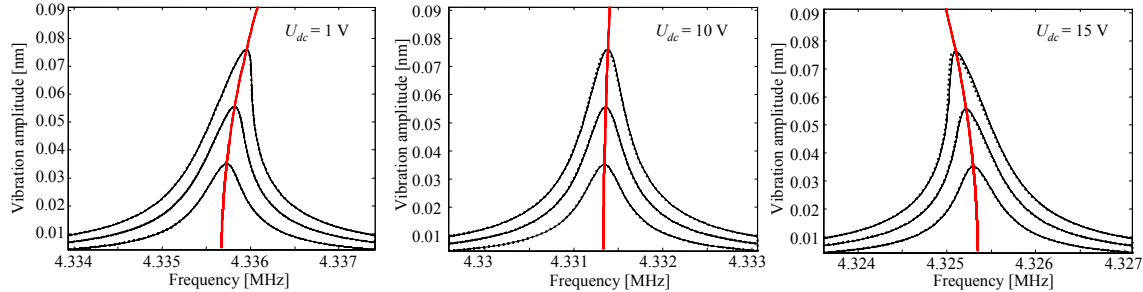


Figure 5. Simulated (dotted lines) and analytical (solid lines) responses for the beam example.

References

- [1] V. Kaajakari, T. Mattila, A. Oja, and H. Seppä, Nonlinear limits for single-crystal silicon microresonators, IEEE J. of Microelectromechanical Systems 13 (2004) 715-724.
- [2] L. D. Landau and E. M. Lifshitz, Mechanics, 3rd ed., Butterworth-Heinemann, Oxford, 1999.

⁴This is left as an exercise to the reader.